Designation: E2760 – 16

Standard Test Method for Creep-Fatigue Crack Growth Testing[1]

This standard is issued under the fixed designation E2760; the number immediately following the designation indicates the year of original adoption or, in the case of revision, the year of last revision. A number in parentheses indicates the year of last reapproval. A superscript epsilon (ε) indicates an editorial change since the last revision or reapproval.

1. Scope

1.1 This test method covers the determination of creep-fatigue crack growth properties of nominally homogeneous materials by use of pre-cracked compact type, C(T), test specimens subjected to uniaxial cyclic forces. It concerns fatigue cycling with sufficiently long loading/unloading rates or hold-times, or both, to cause creep deformation at the crack tip and the creep deformation be responsible for enhanced crack growth per loading cycle. It is intended as a guide for creep-fatigue testing performed in support of such activities as materials research and development, mechanical design, process and quality control, product performance, and failure analysis. Therefore, this method requires testing of at least two specimens that yield overlapping crack growth rate data. The cyclic conditions responsible for creep-fatigue deformation and enhanced crack growth vary with material and with temperature for a given material. The effects of environment such as time-dependent oxidation in enhancing the crack growth rates are assumed to be included in the test results; it is thus essential to conduct testing in an environment that is representative of the intended application.

1.2 Two types of crack growth mechanisms are observed during creep/fatigue tests: *(1)* time-dependent intergranular creep and *(2)* cycle dependent transgranular fatigue. The interaction between the two cracking mechanisms is complex and depends on the material, frequency of applied force cycles and the shape of the force cycle. When tests are planned, the loading frequency and waveform that simulate or replicate service loading must be selected.

1.3 Two types of creep behavior are generally observed in materials during creep-fatigue crack growth tests: creep-ductile and creep-brittle (**1**)[2]. For highly creep-ductile materials that have rupture ductility of 10 % or higher, creep strains dominate and creep-fatigue crack growth is accompanied by substantial time-dependent creep strains near the crack tip. In creep-brittle materials, creep-fatigue crack growth occurs at low creep ductility. Consequently, the time-dependent creep strains are comparable to or less than the accompanying elastic strains near the crack tip.

1.3.1 In creep-brittle materials, creep-fatigue crack growth rates per cycle or *da/dN*, are expressed in terms of the magnitude of the cyclic stress intensity parameter, ΔK. These crack growth rates depend on the loading/unloading rates and hold-time at maximum load, the force ratio, R, and the test temperature (see Annex A1 for additional details).

1.3.2 In creep-ductile materials, the average time rates of crack growth during a loading cycle, $(da/dt)_{avg}$, are expressed as a function of the average magnitude of the C_t parameter, $(C_t)_{avg}$ (**2**).

NOTE 1—The correlations between $(da/dt)_{avg}$ and $(C_t)_{avg}$ have been shown to be independent of hold-times (**2, 3**) for highly creep-ductile materials that have rupture ductility of 10 percent or higher.

1.4 The crack growth rates derived in this manner and expressed as a function of the relevant crack tip parameter(s) are identified as a material property which can be used in integrity assessment of structural components subjected to similar loading conditions during service and life assessment methods.

1.5 The use of this practice is limited to specimens and does not cover testing of full-scale components, structures, or consumer products.

1.6 This practice is primarily aimed at providing the material properties required for assessment of crack-like defects in engineering structures operated at elevated temperatures where creep deformation and damage is a design concern and are subjected to cyclic loading involving slow loading/unloading rates or hold-times, or both, at maximum loads.

1.7 This practice is applicable to the determination of crack growth rate properties as a consequence of constant-amplitude load-controlled tests with controlled loading/unloading rates or hold-times at the maximum load, or both. It is primarily concerned with the testing of C(T) specimens subjected to uniaxial loading in load control mode. The focus of the procedure is on tests in which creep and fatigue deformation and damage is generated simultaneously within a given cycle. It does not cover block cycle testing in which creep and fatigue

[1] This test method is under the jurisdiction of ASTM Committee E08 on Fatigue and Fracture and is the direct responsibility of Subcommittee E08.06 on Crack Growth Behavior.

Current edition approved Nov. 1, 2016. Published January 2017. Originally approved in 2010. Last previous edition approved in 2010 as E2760–10$^{\varepsilon 2}$. DOI: 10.1520/E2760-16.

[2] The boldface numbers in parentheses refer to the list of references at the end of this standard.

damage is generated sequentially. Data which may be determined from tests performed under such conditions may characterize the creep-fatigue crack growth behavior of the tested materials.

1.8 This practice is applicable to temperatures and hold-times for which the magnitudes of time-dependent inelastic strains at the crack tip are significant in comparison to the time-independent inelastic strains. No restrictions are placed on environmental factors such as temperature, pressure, humidity, medium and others, provided they are controlled throughout the test and are detailed in the data report.

NOTE 2—The term *inelastic* is used herein to refer to all nonelastic strains. The term *plastic* is used herein to refer only to time-independent (that is non-creep) component of inelastic strain.

1.9 The values stated in SI units are to be regarded as standard. The inch-pound units in parentheses are for information only.

1.10 *This standard does not purport to address all of the safety concerns, if any, associated with its use. It is the responsibility of the user of this standard to establish appropriate safety and health practices and determine the applicability of regulatory limitations prior to use.*

2. Referenced Documents

2.1 *ASTM Standards:*[3]

E4 Practices for Force Verification of Testing Machines
E83 Practice for Verification and Classification of Extensometer Systems
E139 Test Methods for Conducting Creep, Creep-Rupture, and Stress-Rupture Tests of Metallic Materials
E177 Practice for Use of the Terms Precision and Bias in ASTM Test Methods
E220 Test Method for Calibration of Thermocouples By Comparison Techniques
E399 Test Method for Linear-Elastic Plane-Strain Fracture Toughness K_{Ic} of Metallic Materials
E467 Practice for Verification of Constant Amplitude Dynamic Forces in an Axial Fatigue Testing System
E647 Test Method for Measurement of Fatigue Crack Growth Rates
E1457 Test Method for Measurement of Creep Crack Growth Times in Metals
E1823 Terminology Relating to Fatigue and Fracture Testing
E2714 Test Method for Creep-Fatigue Testing

3. Terminology

3.1 Terminology related to fatigue and fracture testing contained in Terminology E1823 is applicable to this test method. Additional terminology specific to this standard is detailed in section 3.3. For clarity and easier access within this document some of the terminology in Terminology E1823 relevant to this standard is repeated below (see Terminology E1823, for further discussion and details).

[3] For referenced ASTM standards, visit the ASTM website, www.astm.org, or contact ASTM Customer Service at service@astm.org. For *Annual Book of ASTM Standards* volume information, refer to the standard's Document Summary page on the ASTM website.

3.2 *Definitions:*

3.2.1 *crack-plane orientation*—direction of fracture or crack extension relation to product configuration. This identification is designated by a hyphenated code with the first letter(s) representing the direction normal to the crack plane and the second letter(s) designating the expected direction of crack propagation.

3.2.2 *crack size, a [L]*—principal lineal dimension used in the calculation of fracture mechanics parameters for through-thickness cracks.

3.2.2.1 *Discussion*—In the C(T) specimen, a is the average measurement from the line connecting the bearing points of force application. This is the same as the physical crack size, a_p where the subscript p is always implied.

3.2.2.1 *original crack size, a_o [L]*—the physical crack size at the start of testing.

3.2.3 *specimen thickness, B [L]*—distance between the parallel sides of the specimen.

3.2.4 *net thickness, B_N [L]*—the distance between the roots of the side-grooves in side-grooved specimens.

3.2.5 *specimen width, W [L]*—the distance from a reference position (for example, the front edge of a bend specimen or the force line of a compact specimen) to the rear surface of the specimen.

3.2.6 *force, P [F]*—the force applied to a test specimen or to a component.

3.2.7 *maximum force, P_{max} [F]—in fatigue*, the highest algebraic value of applied force in a cycle. By convention, tensile forces are positive and compressive forces are negative.

3.2.8 *minimum force, P_{min} [F]—in fatigue*, the lowest algebraic value of applied force in a cycle. By convention, tensile forces are positive and compressive forces are negative.

3.2.9 *force ratio (also stress ratio), R— in fatigue*, the algebraic ratio of the two loading parameters of a cycle. The most widely used ratio is as follows:

$$R = \frac{\text{minimum load}}{\text{maximum load}} = \frac{P_{min}}{P_{max}} \tag{1}$$

3.2.10 *force range, ΔP [F]—in fatigue loading*, the algebraic difference between the successive valley and peak forces (positive range or increasing force range) or between successive peak and valley forces (negative or decreasing force range). In constant amplitude loading, the range is given as follows:

$$\Delta P = P_{max} - P_{min} \tag{2}$$

3.2.11 *stress intensity factor, K, K_1, K_2, K_3, K_I, K_{II}, K_{III} [$FL^{-3/2}$]*—the magnitude of the mathematically ideal crack tip stress field (a stress-field singularity) for a particular mode in a homogeneous, linear-elastic body.

3.2.11.1 *Discussion*—For a C(T) specimen subjected to Mode I loading, K is calculated by the following equation:

$$K = \frac{P}{(BB_N)^{1/2}W^{1/2}} f(a/W) \tag{3}$$

$$f = \left[\frac{2+a/W}{(1-a/W)^{3/2}}\right](0.886+4.64(a/W) - 13.32(a/W)^2+14.72(a/W)^3 - 5.6(a/W)^4) \tag{4}$$

3.2.12 *maximum stress intensity factor, K_{max} [$FL^{-3/2}$]—in fatigue*, the maximum value of the stress intensity factor in a cycle. This value corresponds to P_{max}.

3.2.13 *minimum stress intensity factor, K_{min} [$FL^{-3/2}$]—in fatigue*, the minimum value of the stress intensity factor in a cycle. This value corresponds to P_{min} when $R > 0$ and is taken to be 0 when $R \leq 0$.

3.2.14 *stress-intensity factor range, ΔK [$FL^{-3/2}$]—in fatigue*, the variation in the stress-intensity factor during a cycle, that is:

$$\Delta K = K_{max} - K_{min} \tag{5}$$

3.2.15 *yield strength, σ_{YS} [FL^{-2}]*—the stress at which the material exhibits a deviation from the proportionality of stress to strain at the test temperature. This deviation is expressed in terms of strain.

3.2.15.1 *Discussion*—For the purposes of this standard, the value of strain deviation from proportionality used for defining yield strength is 0.2 %.

3.2.16 *cycle—in fatigue*, one complete sequence of values of force that is repeated under constant amplitude loading. The symbol N used to indicate the number of cycles.

3.2.17 *hold-time (t_h)—in fatigue*, the amount of time in the cycle where the controlled test variable (for example, force, strain, displacement) remains constant with time.

3.2.18 *C*(t)*—integral, *C*(t) [$FL^{-1}T^{-1}$]*, a mathematical expression, a line or surface integral that encloses the crack front from one crack surface to the other, used to characterize the local stress- strain rate fields at any instant around the crack front in a body subjected to extensive creep conditions.

3.2.18.1 *Discussion*—The *C*(t)* expression for a two-dimensional crack, in the x-z plane with the crack front parallel to the z-axis, is the line integral (**4**, **5**).

$$C^*(t) = \int_\Gamma \left(W^*(t)dy - T \cdot \frac{\partial \dot{u}}{\partial x}\, ds \right) \tag{6}$$

where:

$W^*(t)$	=	instantaneous stress-power or energy rate per unit volume,
Γ	=	path of the integral, that encloses (that is, contains) the crack tip contour,
ds	=	increment in the contour path,
T	=	outward traction vector on ds,
$\dot{u}$	=	displacement rate vector at ds,
x, y, z	=	rectangular coordinate system, and
$T \cdot \frac{\partial \dot{u}}{\partial x}\, ds$	=	the rate of stress-power input into the area enclosed by Γ across the elemental length ds.

3.2.18.2 *Discussion*—The value of *C*(t)* from this equation is path-independent for materials that deform according to a constitutive law that may be separated into single-value time and stress functions or strain and stress functions of the forms (**1**):

$$\dot{\varepsilon} = f_1(t) f_2(\sigma) \tag{7}$$

$$\dot{\varepsilon} = f_3(\varepsilon) f_4(\sigma) \tag{8}$$

where, f_1–f_4 represent functions of elapsed time, t, strain, ε and applied stress, σ, respectively and $\dot{\varepsilon}$ is the strain rate.

3.2.18.3 *Discussion*—For materials exhibiting creep deformation for which the above equation is path-independent, the *C*(t)*-integral is equal to the value obtained from two, stressed, identical bodies with infinitesimally differing crack areas. This value is the difference in the stress-power per unit difference in crack area at a fixed value of time and displacement rate, or at a fixed value of time and applied force.

3.2.18.4 *Discussion*—The value of *C*(t)* corresponding to the steady-state conditions is called C^*_s. Steady-state is said to have been achieved when a fully developed creep stress distribution has been produced around the crack tip. This occurs when secondary creep deformation characterized by Eq 9 dominates the behavior of the specimen.

$$\dot{\varepsilon}_{ss} = A\sigma^n \tag{9}$$

3.2.18.5 *Discussion*—This steady state in *C** does not necessarily mean steady state crack growth rate. The latter occurs when steady state damage develops at the crack tip.

3.2.19 *force-line displacement due to creep, elastic, and plastic strain V [L]* —the total displacement measured at the loading pins (V^{LD}) due to the initial force placed on the specimen at any instant and due to subsequent crack extension that is associated with the accumulation of creep, elastic, and plastic strains in the specimen.

3.2.19.1 *Discussion*—The force-line displacement associated with just the creep strains is expressed as V_c.

3.2.19.2 *Discussion*—In creeping bodies, the total displacement at the force-line, V^{FLD}, can be partitioned into an instantaneous elastic part V_e, a plastic part, V_p, and a time-dependent creep part, V_c (**6**).

$$V \approx V_e + V_p + V_c \tag{10}$$

The corresponding symbols for the rates of force-line displacement components shown in Eq 10 are given respectively as $\dot{V}$, $\dot{V}_e$, $\dot{V}_p$, $\dot{V}_c$. This information is used to derive the parameters C^* and C_t.

3.2.20 *C_t parameter, C_t [$FL^{-1}T^{-1}$]*—parameter equal to the value obtained from two identical bodies with infinitesimally differing crack areas, each subjected to stress, as the difference in stress power per unit difference in crack area at a fixed value of time and displacement rate or at a fixed value of time and applied force for an arbitrary constitutive law (**5**).

3.2.20.1 *Discussion*—The value of C_t is path-independent and is identical to *C*(t)* for extensive creep conditions when the constitutive law described in section 3.1.18.2 of *C*(t)-integral* definition applies.

3.2.20.2 *Discussion*—Under small-scale creep conditions, *C*(t)* is not path-independent and is related to the crack tip stress and strain fields only for paths local to the crack tip and well within the creep zone boundary (**7**). Under these circumstances, C_t, is related uniquely to the rate of expansion of the creep zone size (**7**). There is considerable experimental evidence that the C_t parameter which extends the *C* (t)-integral* concept into small-scale and the transition creep regime, correlates uniquely with creep crack growth rate in the entire regime ranging from small-scale to extensive creep regimes (**5**).

3.2.20.3 *Discussion*—For a specimen with a crack subject to constant force, P and under a small-scale-creep (**5**):

$$C_t = \frac{P\dot{V}_c}{BW}\,(f'/f) \tag{11}$$

and

$$f' = \frac{df}{d(a/W)} \quad (12)$$

3.2.21 *creep zone boundary*—the locus of points ahead of the crack tip where the equivalent strain caused by the creep deformation equals 0.002 (0.2 %) (**8**).

3.2.21.1 *Discussion*—Under small-scale creep conditions, the creep zone expansion with time occurs under self-similar manner for planar bodies (**9**), thus, the creep zone size, r_c, can be defined as the distance of the creep zone boundary from the crack tip at a fixed angle, θ, with respect to the crack plane. The rate of expansion of the creep zone size is designated as $\dot{r}_c(\theta)$.

3.3 *Definitions of Terms Specific to This Standard:*

3.3.1 $(C_t)_{avg}$ *parameter,* $(C_t)_{avg}$ $[FL^{-1}T^{-1}]$—the average value of the C_t parameter during the hold-time of the cycle and is given by (**1, 2**):

$$(C_t)_{avg} = \frac{1}{t_h}\int_0^{t_h} C_t dt \quad (13)$$

where:

t_h = hold-time at maximum load measured from the start of the hold period.

Eq 13 can also be written as:

$$(C_t)_{avg} = \frac{P_{max}(\Delta V_c)}{(BB_N)^{1/2} W t_h}(f'/f) \quad (14)$$

where:

ΔV_c = the difference in the force-line displacement between the end and the start of the hold-time during a cycle (**1**).

3.3.1.1 *Discussion*—The value of $(C_t)_{avg}$ from Eq 14 is appropriate for small-scale creep regime but it's value is identical to the value of $C^*(t)$ for extensive creep conditions when the constitutive law described in section 3.2.18 is applicable.

3.3.2 *creep-fatigue crack growth rate behavior (CFCGR):*

for creep-ductile materials, this is a plot of the incremental, average time rate of crack growth, $(da/dt)_{avg}$, as a function of $(C_t)_{avg}$.

for creep-brittle materials, this is a plot of incremental crack growth rate per loading cycle, *da/dN*, as a function of the cyclic stress intensity factor, Δ*K*, for constant temperature, hold-time, and force ratio, *R*.

3.3.3 *transition time,* t_T *[T]*—time required for extensive creep conditions to develop in a cracked body (**9**). For specimens, this is typically the time required for the creep deformation zone to spread through a substantial portion of the uncracked ligament, or in the region that is under the influence of a crack in the case of a finite crack in a semi-infinite medium.

3.3.3.1 *Discussion*—An estimate of transition time for materials that creep according to the power-law can be obtained from the following equation(**9**):

$$t_T = \frac{K^2(1-\nu^2)}{E(n+1)C^*} \quad (15)$$

where:

ν = Poisson's ratio, and

n = secondary creep exponent as in Eq 9.

3.3.4 *force-line compliance* (C_{FL})—the elastic displacement in the specimen along the force-line divided by the force. This value is uniquely related to the normalized crack size of the specimen.

3.3.5 *force line displacement rate due to creep,* $\dot{V}_c$ $[LT^1]$—rate of increase of the force-line displacement due to creep strains.

4. Significance and Use

4.1 Creep-fatigue crack growth testing is typically performed at elevated temperatures over a range of frequencies and hold-times and involves the sequential or simultaneous application of the loading conditions necessary to generate crack tip cyclic deformation/damage enhanced by creep deformation/damage or vice versa. Unless such tests are performed in vacuum or an inert environment, oxidation can also be responsible for important interaction effects relating to damage accumulation. The purpose of creep-fatigue crack growth tests can be to determine material property data for *(a)* assessment input data for the damage condition analysis of engineering structures operating at elevated temperatures, *(b)* material characterization, or *(c)* development and verification of rules for design and life assessment of high-temperature components subject to cyclic service with low frequencies or with periods of steady operation, or a combination thereof.

4.2 In every case, it is advisable to have complementary continuous cycling fatigue data (gathered at the same loading/unloading rate), creep crack growth data for the same material and test temperature(s) as per Test Method E1457, and creep-fatigue crack formation data as per Test Method E2714. Aggressive environments at high temperatures can significantly affect the creep-fatigue crack growth behavior. Attention must be given to the proper selection and control of temperature and environment in research studies and in generation of design data.

4.3 Results from this test method can be used as follows:

4.3.1 Establish material selection criteria and inspection requirements for damage tolerant applications where cyclic loading at elevated temperature is present.

4.3.2 Establish, in quantitative terms, the individual and combined effects of metallurgical, fabrication, operating temperature, and loading variables on creep-fatigue crack growth life.

4.4 The results obtained from this test method are designed for crack dominant regimes of creep-fatigue failure and should not be applied to cracks in structures with wide-spread creep damage. Localized damage in a small zone around the crack tip is permissible, but not in a zone that is comparable in size to the crack size or the remaining ligament size.

5. Functional Relationships

5.1 Empirical relationships that have been commonly used for description of creep-fatigue crack growth data are given in Annex A1. These relationships typically have limitations with

respect to material types such as high temperature ferritic and austenitic steels (creep-ductile materials) versus nickel base alloys (typically creep-brittle materials). Therefore, original data should be reported to the greatest extent possible. Data reduction methods should be detailed along with assumptions. Sufficient information should be recorded and reported to permit analysis, interpretation, and comparison with results for other materials analyzed using currently popular methods.

6. Apparatus

6.1 *Testing Machine*—Tests shall be conducted using a servo-controlled tension-compression fatigue machine that has been verified in accordance with Practices E4 and Practice E467. Hydraulic and electromechanical machines are acceptable. The complete loading system comprising force transducer, specimen clevises and test specimen shall have lateral rigidity and be capable of executing the prescribed cycle in force control. It shall be possible to measure the response variable, extension, to the required tolerances. Further, auxiliary equipment for measuring crack size as a function of cycles to the required tolerances shall be available as part of the apparatus.

6.2 *Force Transducer:*

6.2.1 The force transducer shall be designed for tension-compression fatigue testing and shall have high axial and lateral rigidity. Its capacity shall be sufficient to measure the axial forces applied during the test to an accuracy better than 1 % of the reading. The force transducer and its associated electronics shall comply with Practices E4 and Practice E467.

6.2.2 The force transducer shall be temperature compensated and not have zero drift nor sensitivity variation greater than 0.002 % of the full scale per degree Celsius. During test, the force transducer shall be maintained at a temperature within its temperature compensation range. Force transducers are subject to thermal drift in zero point and sensitivity and may be permanently damaged by temperatures in excess of 50°C. Suitable cooling arrangements include forced air cooling of fins at the outer ends of the loading bars or water cooling coils or jackets. Care should be taken to ensure that force transducer calibration and force train alignment are not affected by the presence of the cooling devices.

6.3 *Alignment of Grips*—It is important that attention be given to achieving good alignment in the force-line through careful machining of all gripping fixtures. The length of the force train should be chosen with proper attention to the height of the furnace for heating the test specimen. The loading train should incorporate cooling arrangements to limit heat transfer from the hot zone to the testing machine and in particular the force transducer.

6.4 *Heating Apparatus:*

6.4.1 The apparatus for, and method of, heating the specimens should provide the temperature control necessary to satisfy the requirements in section 9.6.4, without manual adjustments more frequently than once in each 24-h period after force application.

6.4.2 Heating shall be by an electric resistance or radiation furnace with the specimen in air at atmospheric pressure unless other media are specifically agreed upon in advance.

6.5 *Displacement Gage for the Measurement of the Force Line Displacement During the Test:*

6.5.1 Continuous force-line displacement measurement is needed to evaluate the magnitude of $(C_t)_{avg}$ as a function of creep-fatigue cycles during the test in creep-ductile materials. Displacement measurements must be made on the force-line. As a guide, the displacement gage should have a working range no more than twice the displacement expected during the test. Accuracy of the gage should be within ±1 % of the full working range of the gage. In calibration, the maximum deviation of the individual data points from the fit to the data shall not exceed ±1 % of the working range.

NOTE 3—Thermal effects, particularly thermal gradients, can change extensometer output and must be minimized. It is good practice to keep the body of the extensometer outside the furnace unless it is designed to withstand the test temperature.

6.5.2 Knife edges are recommended for friction-free seating of the gage. Parallel alignment of the knife edges must be maintained to within ±1°.

6.5.3 The displacement along the force-line may be directly measured by attaching the entire clip gage assembly to the specimen and placing the whole assembly in the furnace. Alternatively, the displacements can be transferred outside the furnace with ceramic rods. In the latter procedure, the transducer is placed outside the furnace. Other designs that can measure displacements to the same levels of accuracy may also be used.

6.5.4 The extensometer used shall be suitable for measuring force-line displacements over long periods during which there shall be minimal drift, slippage and instrument hysteresis. Extensometers used for measurement shall be suitable for dynamic measurements over periods of time, i.e. should have a rapid response and with a low hysteresis (not greater than 0.1 % of extensometer output). Strain gauge, capacitance gauge, DCDT or LVDT type transducers are generally used and should be calibrated according to Practice E83. The extensometer should meet the requirements of Grade B2 or better as specified by Practice E83.

6.6 *Crack Monitoring:*

6.6.1 A direct current (DCPD) or alternating current (ACPD) electrical potential-drop crack monitoring system must be used. Further details on the attachment of the input and output electrical leads and measurement procedures are given in Annex A2.

NOTE 4—It is good practice to electrically insulate the test specimen (or loading grips) from the test machine loading frame and ancillary equipment in order to avoid unstable potential drop recordings associated with earth loops. However, it is not essential to do so. The contact resistance between the loading pin holes and the pins can provide sufficient electrical insulation.

6.6.2 The DCPD or ACPD system should be capable of reliably resolving crack extensions of at least ±0.1 mm at the test temperature.

6.7 *Temperature Measurement and Control*—Test specimen temperature shall be measured using Class 1 thermocouples in contact with the test specimen surface in the region near the crack plane. In all cases involving the use of thermocouples, it is essential to ensure that intimate thermal contact is achieved

between test specimen and thermocouple without affecting the properties of the test specimen. When using furnace heating, thermocouple beads shall be shielded from direct radiation.

NOTE 5—For long duration creep-fatigue tests, the use of Type K thermocouples above 400°C is not recommended. Their use for short duration tests (<500 h) at temperatures up to 600°C is possible, but their re-use is not recommended in these circumstances. Similarly, Type N thermocouples may be used for short duration tests (<500 h) at temperatures up to 800°C, with their re-use not being recommended without recalibration.

6.8 *Cycle Counter*—Standard practice should be to record all cycles in a data acquisition system. As a minimum, a digital device should be used to record the number of cycles applied to the test specimen. Five digits are required. For tests lasting less than 10 000 cycles, individual cycles shall be counted. For longer tests, the device shall have a resolution better than 1 % of the actual life.

6.9 *Data Recording*—An automatic digital recording system should be used which is capable of collecting and simultaneously processing the force, force-line displacement, DCPD or ACPD and temperature data as a function of time and cycles. The sampling frequency of the data shall be sufficient to ensure correct definition of the loading cycle. In particular, it should be sufficient to identify values of load and extension at taming points in the loading diagram, e.g. at cycle maxima and minima, and start and end of hold-time values.

NOTE 6—At least 200 data points should be collected to define the loading and unloading segments of the cycle and an additional 100–200 data points should be collected to fully characterize hold-time duration.

NOTE 7—The simultaneous recording of servo position is also recommended to assist in the retrospective diagnosis of disturbances during test, e.g. extensometer slippage.

7. Test Specimen

7.1 The schematic and dimension of the C(T) specimen is shown in Fig. 1.

NOTE 8—The crack mouth geometry and dimensions and the machine notch and knife edge configuration may be varied from the one in Fig. 1 to adapt to the clip gage chosen for measuring force-line displacements.

7.2 The width-to-thickness ratio *W/B* for the C(T) specimen is recommended to be 4, nominally. Other *W/B* ratios, up to 8, may be used for thickness effect characterization or to reduce forces during the test; it is however important to note that the stress state may vary with thickness.

7.3 The initial crack size, a_0 (including a sharp starter notch or pre-crack), shall be at least 0.25 times the width, *W*, but no greater than 0.35*W*. This may be varied within the stated interval depending on the selected force level for testing and the desired test duration.

7.4 *Specimen Size*—Specimen size must be chosen with consideration to the material availability, capacity of the loading system, being able to fit the specimen into the heating furnace with sufficient room for attaching the necessary extensometers, and providing sufficient ligament size for growing the crack in a stable fashion to permit collection of crack

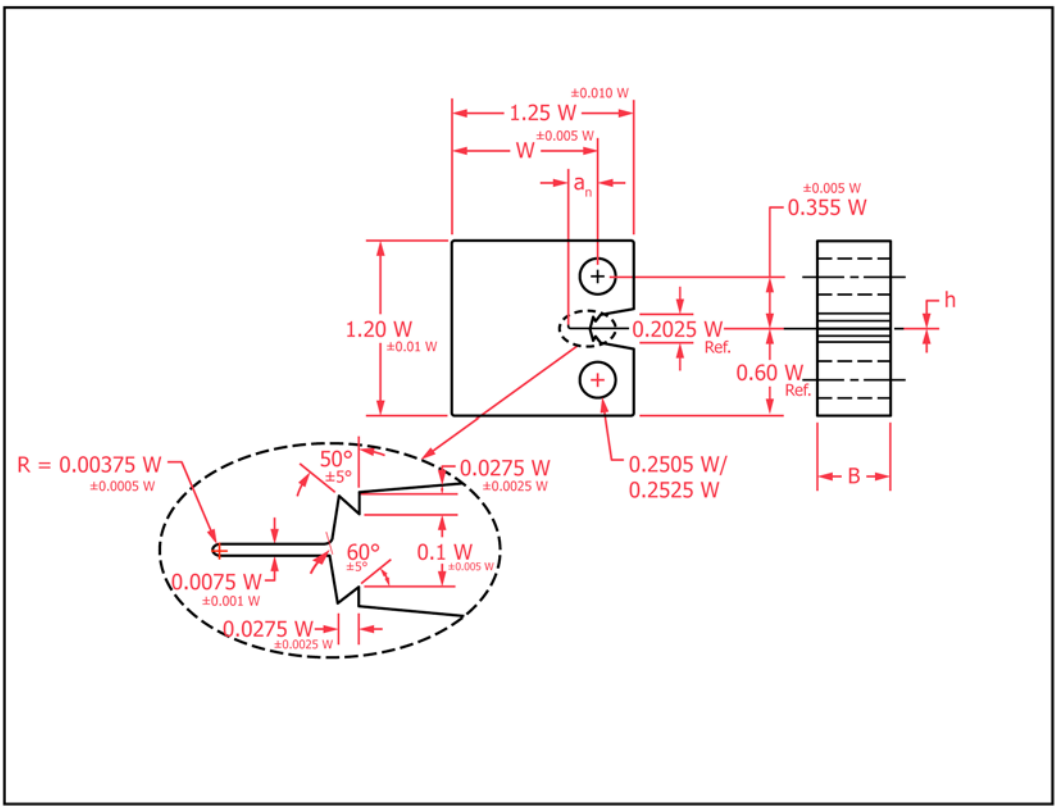

FIG. 1 Drawing of a C(T) Specimen Recommended for Creep-Fatigue Crack Growth Testing and the Details of the Machined Notch and the Knife-Edges for Securely Attaching the Extensometer

growth data. Specimen size requirements to maintain dominantly elastic conditions in the specimen to validate the creep-fatigue crack growth data are addressed in section 10.3.2.

7.5 *Specimen Measurements*—Specimen dimensions are given in Fig. 1. They shall be machined within the machining tolerances specified and the dimensions should be measured before commencing the test.

7.6 *Notch Preparation*—The machined notch for the test specimens may be made by electrical-discharge machining (EDM), milling, broaching, or saw cutting. It is recommended that the last 0.1 *a/W* of the crack be machined using electro-discharge machining (EDM) of a width of 0.1 mm. This will allow easier pre-cracking or further crack tip sharpening by EDM to the final crack starter size prior to testing.

7.7 *Pre-cracking*—Fatigue pre-cracking is used to introduce a sharp starter crack; it is recommended that a narrow slit (of 0.1 mm width) ahead of the machined notch be introduced using electro-discharge machining (EDM) prior to fatigue pre-cracking. This ensures that the final crack front is straight and flat and does not deviate from the crack plane. In creep-brittle materials, EDM notch itself may be used as the pre-crack due to difficulties in growing cracks with straight fronts. If there are indications that the mode of pre-cracking has affected the initial CFCG data, such data must be excluded from being reported as valid data.

NOTE 9—If unusual crack growth trends are observed during the first 0.25 mm of crack extension, the data could be excluded as being invalid CFCG rate or at the very least flagged as being suspect due to possible transient effects.

7.7.1 Care must be exercised during fatigue pre-cracking to avoid excessive damage at the notch root. Hereafter, the method for pre-cracking is described.

7.7.2 *Fatigue pre-cracking:*

7.7.2.1 Specimens may also be pre-cracked at room temperature or at a temperature between ambient and test temperature under fatigue forces to be estimated from the following equation:

$$\frac{\Delta K}{E} \le 0.08 \times 10^{-3}\sqrt{m}\left(0.5 \times 10^{-3}\sqrt{\text{in.}}\right) \tag{16}$$

7.7.2.2 Fatigue pre-cracking is conducted at a load ratio, *R*, of 0.1 or higher using any convenient loading frequency. The accuracy of the fatigue force value shall be within ±5 %. The stress intensity factor range, ΔK, may be calculated using Eq 3 and Eq 4.

7.7.3 The maximum force during the last 0.5 mm (0.02 in.) of crack extension must not exceed the maximum force used during creep-fatigue crack growth testing.

7.7.4 To facilitate fatigue pre-cracking at low stress ratios, the machined notch root radius can be approximately 0.075 mm (0.003 in.). It may at times be expedient to have an EDM notch of 0.1 mm width to enhance the fatigue crack growth. A chevron form of machined notch as described in Test Method E399 or pre-compression of the straight through notch as described in Test Method E399 may be helpful when control of crack shape is a problem.

7.7.5 Pre-cracking is to be done with the material in the same heat-treated condition as that in which it will be tested for creep-fatigue crack growth behavior. No intermediate heat treatments between pre-cracking and testing are allowed.

7.7.6 The size of the pre-crack extension from the machined notch shall be no less than 0.05 *a/W*.

7.8 *Specimen Preparation for Electric Potential Measurement*—The potential drop could be AC or DC powered. The input should be remote from the crack and welded to the specimen. The specific recommendations for the C(T) specimen is presented in Annex A2. For gripping fixtures and wire selection and attachment also refer to the Annex in Test Method E647.

7.9 *Attachment of Thermocouples and Input Leads:*

7.9.1 A thermocouple must be attached to the specimen for measuring the specimen temperature. The thermocouple should be located in the uncracked ligament region of the specimen 2 to 5 mm (0.08 to 0.2 in.) above or below the crack plane. Multiple thermocouples are recommended for specimens wider than 50 mm (2 in.). These thermocouples must be evenly spaced over the uncracked ligament region above or below the crack plane as stated above.

7.9.2 In attaching thermocouples to a specimen, the junction must be kept in intimate contact with the specimen and shielded from radiation, if necessary. Shielding is not necessary if the difference in indicated temperature from an unshielded bead and a bead inserted in a hole in the specimen has been shown to be less than one half the permitted variations in section 9.6.4. The bead should be as small as possible and there should be no shorting of the circuit (such as could occur from twisted wires behind the bead). Ceramic insulators should be used in the hot zone to prevent such shorting.

7.9.3 Specifications in Test Methods E139 identify the type of thermocouples that may be used in different temperature regimes. It is important to note that creep-fatigue crack growth test durations are invariably long. Thus, a stable temperature measurement method should be used to reduce experimental error.

8. Calibration and Standardization

8.1 Performance of the electric potential system, the force measuring system, the temperature measurement systems and the displacement gage must be verified. Calibration of these devices should be as frequent as necessary to ensure that the errors for each test are less than the permissible indicated variations cited in this standard. The testing machine should be calibrated at least annually or, for tests that last for more than a year, after each test. Instruments in constant (or nearly constant) use should be calibrated more frequently; those used occasionally must be calibrated before each use.

8.1.1 Calibrate the force measuring system according to Practices E4.

8.1.2 Calibrate the displacement gage according to Practice E83.

8.1.3 Verify electric potential system according to guidelines in and recommendation in Annex A2.

8.1.4 Calibrate the thermocouples according to Test Method E220.

9. Procedure

9.1 *Plans for a Test Matrix*—A test matrix should be set up identifying, as far as possible, the goals for the tests such as the planned test times, available specimens, number of tests and the force levels that may be needed for the tests. At least one duplicate test shall be conducted such that all test conditions are nominally the same except the applied force ranges. The differences in the applied force ranges between the two tests shall be such that the crack growth ranges are extended with respect to each other and the overlap in the crack growth rates between the tests is no more than one-third of the combined crack growth rate range covered by the two tests. Availability of spare specimens is essential as repeat tests may be required in some instances.

9.2 *Number of Tests*—Creep-fatigue crack growth rate data exhibit scatter. The $(da/dt)_{avg}$ values at a given value of $(C_t)_{avg}$ for creep-ductile materials and da/dN versus ΔK for creep-brittle materials can vary by as much as a factor of 2 to 3 if all other variables such as geometry, specimen size, crack size, loading method and temperature are kept constant. This scatter may increase further by variables such as microstructural differences, force precision, environmental control, and data processing techniques. Therefore, it is good practice to conduct replicate tests whenever practical. Confidence in the inferences drawn from the data will increase with the number of tests and the number of tests will depend on the end use of the data.

9.3 *Specimen Installation*—Install the specimen on the machine by inserting both pins, then apply a small force (approximately 10 % of the intended test force) to remove slack from the loading train. Connect the current input and voltage leads to the current source and voltmeter, respectively. Attach the displacement gage to the specimen and the thermocouple to the appropriate potentiometer. Bring furnace into position and start heating the specimen.

9.4 *Heating the Test Specimen*—The test specimen shall be heated to the specified temperature and shall be maintained at that temperature for at least 30 minutes before loading. During heating, the temperature of the test specimen shall not exceed the specified temperature within its tolerances. A small preload equal to about 10 % of the maximum test load should be applied to the specimen during heating to ensure that the loading train remains under tension at all times.

9.5 *Cycle Shape*—The cycle shape that shall be used for creep-fatigue crack growth testing include *(a)* low frequency triangular wave forms with low control parameter ramp rates, *(b)* saw-tooth wave forms in which the ramp rate of the tensile-going transient is significantly different to that of the unloading portion, and *(c)* cyclic/hold forms comprising a series of ramps with hold-time(s) at the maximum load (the ramp rates may not always be the same). Example creep-fatigue cycle shapes are shown in Fig. 2. There are many other possibilities depending on the practical application for which the creep-fatigue data are required.

9.6 *Starting and Conducting the Test:*

9.6.1 The extensometer output should be brought to a null value with no force on the test specimen. A force to not exceed $0.5P_{max}$ should be applied in increments and the displacement and the PD should be monitored to ensure that the extensometer is properly seated and the PD system is working well and the information is available for post test analysis. The time for application of the force should be as short as possible within these limitations.

9.6.2 The compliance of the specimen should be recorded by manually applying loads that do not exceed $0.5P_{max}$. Three compliance measurements should be made and the average of the three readings should be within 15 % of the theoretical value for the specimen. The relationship between compliance and crack size for measurements made at the load-line are given by the following equation (**10**):

$$C_{FL} = \frac{V_{FI}}{P} = \frac{1}{E(BB_N)^{1/2}}\left[\frac{W+a}{W-a}\right]^2 [12.1630 + 12.219(a/W) - 20.065(a/W)^2 - 0.9925(a/W)^3 + 20.609(a/W)^4 - 9.9314(a/W)^5] \quad (17)$$

9.6.3 Choose the appropriate cyclic force range that will give the desired crack growth rate range. This estimate can be made from previous tests under similar conditions if available or estimated from available data in the literature on similar

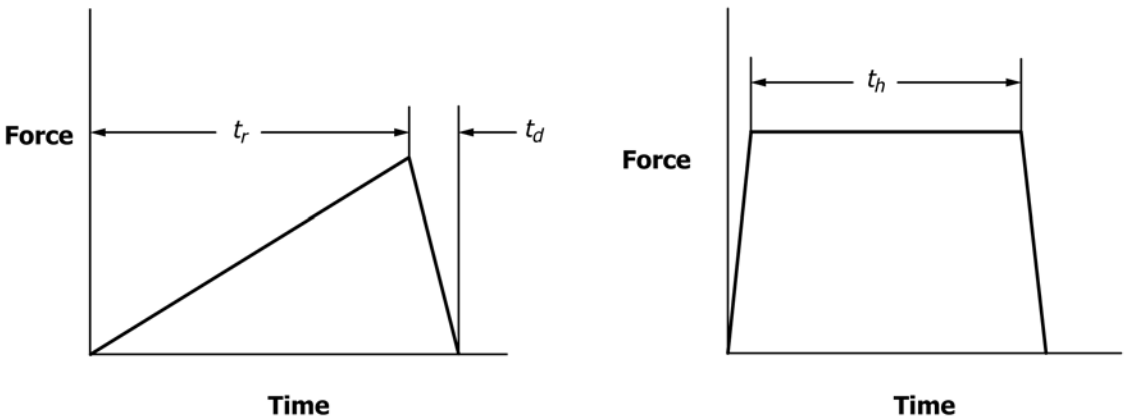

FIG. 2 Example Creep-Fatigue Cycle Shapes

materials. If none is available the first test should be tested with incremental force increases to identify the appropriate force levels.

9.6.4 Before the test force is applied and for the duration of the test, do not permit the difference between the indicated temperature and the nominal test temperature to exceed the following limits: Up to and including 1000°C (1832°F) ± 2°C (± 3°F) above 1000°C (1832°F) ± 3°C (± 5°F). The term "indicated temperature" means the temperature indicated by the temperature measuring device using good quality pyrometric practice.

NOTE 10—It is recognized that the true temperature may vary more than the indicated temperature. Permissible indicated temperature variations are not to be construed as minimizing the importance of good pyrometric practice and precise temperature control. All laboratories should keep indicated and true temperature variations as small as practical. It is well recognized, in view of the extreme dependency of material properties to temperature, that close temperature control is necessary. The limits prescribed represent ranges that reflect common practice.

9.6.4.1 The time for holding at temperature prior to start of test should be governed by the time necessary to ensure that the temperature can be maintained within the limits specified in 9.6.4. This time will not be less than one hour per 25 mm (1 in.) of specimen thickness. Report the time to attain test temperature and the time at temperature before loading.

9.6.4.2 Any positive temperature excursion beyond the limits specified in 9.6.4 is cause for rejection of the test. Negative temperature excursions wherein temperature falls below the specified limits should not be cause for rejection. Low temperatures do not induce the potentially adverse material changes associated with elevated temperatures. It is recommended that the crack growth data obtained during the low temperature excursion and during the period corresponding to 0.5 mm (0.02 in.) of crack extension following stabilization of the temperature be considered invalid and excluded.

9.6.5 The current for the electric potential system should be turned on at the same time as the furnace. This is necessary to ensure that resistance heating of the specimen caused by the applied current also stabilizes as the specimen is brought up to the test temperature.

9.6.5.1 Prior to starting the test, the initial electric potential voltage output should be measured. If constant current DCPD is used the voltage output should be measured for both current on and current off positions.

NOTE 11—The initial output voltage in the current off position corresponds to the thermal electromotive force (thermal EMF) which must be subtracted from the voltage output before relating the change in voltage to crack extension. This is not necessary if the current is cycled between on and off positions and the change in voltage corresponding to the on and off positions is used for determining crack extension.

9.6.6 Begin the test by applying the minimum force on to the specimen and then subjecting it to the desired cyclic forces.

9.7 *Measurements During the Test:*

9.7.1 The electric potential voltage, force, force-line displacement, and test temperature should be recorded continuously during the test. The force and temperature records are retained to ensure that these control parameters remain within their prescribed limits at all times during the test. At the start of test, a continuous recording shall be made of the initial values of the electric potential voltage and the displacement. During the course of test, periodic recording is sufficient. The frequency of these recordings shall be chosen appropriately for the expected overall duration of the test.

NOTE 12—It is common to continuously record the data from the first 5 cycles and then for cycles at logarithmic intervals (that is, 16, 25, 40, 63, 100, 160, etc.). If data acquisition is automated, the acquisition of electric potential and displacement output as a function of time may be programmed either with a predefined interval or as a function of the progression of each of the two parameters (force and extension). In either case, the sampling frequency shall be sufficient to allow clear definition of their variation during the cycle.

9.7.2 The test should be stopped when both the potential drop and the displacement measurement indicate that rapid crack growth has begun and that final failure of the specimen is imminent. This region can be estimated from continuous monitoring of the data when the displacement and the PD are both increasing rapidly in relation to the immediate past period. It is highly recommended to terminate a test prior to fracture because the final crack front is delineated more clearly and can be accurately measured for verifying the potential drop measurement. It will also allow for better metallographic analysis.

NOTE 13—As a guidance, when the crack growth rate exceeds 2.5×10^{-2} mm/cycle, the test should shut down. This condition is met approximately when:

$$\frac{1}{U}\left(\frac{dU}{dN}\right) \geq \frac{10^{-2}}{a_0} \tag{18}$$

where:

U = the instantaneous value of the PD,
N = the number of fatigue cycles, and
a_0 = the original crack size in mm.

9.8 *Post-test Measurements:*

9.8.1 When the test is complete or stopped, remove the force and turn off the furnace. After the specimen has cooled down, remove the specimen from the machine without damaging the fracture surface.

9.8.2 If the specimen did not fracture at the end of the test, it should be broken open taking care to minimize additional permanent deformation. The use of cyclic force to break open the specimen is recommended. Also, ferritic steels may be cooled to a temperature below the ductile-brittle transition and fractured.

9.8.3 Along the front of the pre-crack and the front of the marked region of creep-fatigue crack growth, measure the crack size at five equally spaced points centered on the specimen mid-thickness line. Calculate the original crack size, a_0, and the final crack size, a_f, by calculating the average of the five measurements along the crack front. The measuring instrument shall have a minimum accuracy of 0.025 mm.

10. Calculation Procedure

10.1 *Determination of Crack Size*—Prior to applying the procedure described in Annex A2 for determining the crack size during the test as a function of fatigue cycles it is recommended to perform the following actions:

10.1.1 Determine the shape of the crack front at the start and end of the test using the measurements described in section 9.8.3.

NOTE 14—If the variation in crack size at any point along the crack front is more than ±10 % of the average value, the results are not reliable. Using side-grooves in future testing is highly recommended.

10.1.2 Calculate the crack extension, Δa_t, by subtracting the observed initial crack size, a_0, from the value of the observed final crack size, a_f. The final crack size shall be determined from surface fractography measurements where possible.

10.1.3 Calculate crack growth with cycles as shown in Annex A3. The crack size can be determined by linear interpolation of the electric potential readings using the initial crack size, a_0, and the final crack size, a_f. The intervals between successive data points must be selected such that the crack increment lies between 0.25 mm to 0.5 mm.

10.1.4 If failure of the specimen occurs prior to stopping the test then fractography measurements of the final crack size may not be possible. In this case follow the procedure described in A2.2 using the predictive formula to estimate the crack size as a function of fatigue cycles. It is then recommended that measurements from tests in question be compared with other valid data under similar conditions prior to inclusion in the data set.

10.2 *Calculation of the Appropriate Displacement Rate*—The average displacement rate $(dV/dt)_{avg}$ during the hold-time is recommended to be used in the determination of $(C_t)_{avg}$. However, this is only valid if the changes in force-line displacement, ΔV, during hold time are dominated by creep deformation. The procedure for determining whether this condition is met is described in 10.3.2.

10.3 *Calculation of the ΔK and $(C_t)_{avg}$ Parameters:*

10.3.1 Eq 3 and Eq 14 give the details for the recommended solutions for determining ΔK and $(C_t)_{avg}$ respectively. It is evident from the literature that there are varying techniques available for the evaluation of ΔK and $(C_t)_{avg}$. The differences that may be observed in terms of ΔK are usually not greater than ±1 %. However due to the high stress sensitivity in the creep process, these differences can be considerably larger when comparing different $(C_t)_{avg}$ evaluation methods especially in the absence of accurate force-line displacement measurements.

10.3.2 *Valid and Recommended Solutions*—The optimum method for estimating $(C_t)_{avg}$ for C(T) specimens have been presented in section 3.3.1. The following procedure is necessary to determine if the creep-fatigue crack growth rates should be expressed as da/dN versus ΔK for a fixed hold-time as is the case for creep-brittle materials or if they should be expressed as $(da/dt)_{avg}$ versus $(C_t)_{avg}$. The total measured change in force-line displacement, ΔV, can be partitioned into an instantaneous (elastic) part, ΔV_e, and a time-dependent part that is directly associated with the accumulation of creep strains, ΔV_c, using the following equation for estimating ΔV_e **(6)**:

$$\Delta V_e = \frac{t_h \left(\frac{da}{dt}\right)_{avg}}{P} B \left[\frac{2\Delta K^2}{E'}\right] \quad (19)$$

where:

$(da/dt)_{avg}$ = the crack growth rate,
P = the applied force,
B = the specimen thickness,
ΔK = the stress intensity factor, and
E' = the effective elastic modulus ($E/(1–\nu^2)$ for plane strain and E for plane stress.

10.3.2.1 For side-grooved specimens, B in Eq 19 should be replaced by B_N. Thus by deriving ΔV_e from Eq 17 and by comparing it to the measured value of ΔV during the hold-time, a determination can be made about creep-ductile versus creep-brittle behavior. If $\Delta V_e \leq 0.5\ \Delta V$, the material will be considered as creep-ductile and if $\Delta V_e > 0.5\ \Delta V$, creep-brittle conditions are expected to prevail.

10.4 If, during the test, the crack deviates outside an envelope that encompasses the material between the planes that are oriented at ±5° from the idealized plane of crack growth and that intersect the axis of loading, the data are invalid by this test method. It is therefore recommended that the test geometry should be changed or side-grooving considered, or both.

10.5 Data acquired after the accumulated force-line deflection, exceeds $0.05W$, which could be due to either creep or plasticity, are considered invalid by this test method.

11. Report of Findings

11.1 Report the following information:

11.1.1 Specimen type and dimensions including thickness, B, net thickness, B_N (if side-grooved) and width, W.

11.1.2 Description of the test machine and equipment used to measure crack size and the precision with which crack size measurements were made.

11.1.3 Test material characterization in terms of the heat treatment, chemical composition, tensile properties at room temperature and test temperature, the pre-exponent A and the creep exponent n (for the Norton relationship giving the creep strain rate $\dot{\varepsilon} = A\sigma^n$) used in calculations, including how it was derived. Also identify product size and form (for example, sheet, plate, and forging),

11.1.4 *Crack Plane Orientation*—In addition, if the specimen is removed from a large product form, give its location with respect to the parent.

11.1.5 The terminal value of ΔK, P_{max}, P_{min}, the pre-cracking temperature, and the frequency of loading and the number of cycles used for fatigue pre-cracking. If pre-crack forces were stepped-down, state the procedure employed for the loading method and give the amount of crack extension at the final force level. If an EDM notch is used in-lieu of a fatigue pre-crack, report the root radius and the length of the notch.

11.1.6 State test force and experimental variables such as test temperature and environment. For environments other than laboratory air, report the chemical composition and partial pressures of the gases.

11.1.7 Report the data analysis methods, including the technique used to convert crack size and deflection data into rates and the specific procedure used to correct for discrepancies between measured crack extension on the fracture surface with that predicted from the electric potential method.

11.1.8 Plot $(da/dt)_{avg}$, versus $(C)_{avg}$ or da/dN versus ΔK. It is recommended that $(C_t)_{avg}$ or ΔK be the abscissa and

$(da/dt)_{avg}$ or da/dN be the ordinate. Log-Log coordinate axes are normally used. Report all data that violate the validity criteria in 10.1 – 10.5 and identify.

12. Precision and Bias

12.1 *Precision*—The precision of $(da/dt)_{avg}$ versus $(C_t)_{avg}$ or da/dN versus ΔK at a fixed hold-time is a function of inherent material variability as well as errors in measuring crack size, temperature, creep displacement rates and applied force levels. It is often impossible to separate the contributions from each of the above mentioned sources of variability so an overall measure of variability can be obtained to determine precision as per Practice E177.

NOTE 15—It is important to recognize that for the purposes of design or remaining life assessment, inherent material variability often becomes the primary source of scatter in the crack growth rates. The variability associated with a given lot of material is caused by inhomogenities in chemical composition, micro structure and the local creep properties, or all of the above. The same factors coupled with varying processing conditions give rise to further batch to batch differences in creep-fatigue cracking rates. An assessment of inherent material variability, either within or between heats or lots, can be determined only by conducting a statistically planned test program on the material of interest. Thus, the results from the inter-laboratory test programs utilizing materials selected to minimize material variability allow assessment of measurement precision, but are generally not applicable to questions regarding inherent variability in other materials.

12.2 *Bias*—There is no accepted "standard" value for creep-fatigue crack growth rates for any material.

13. Keywords

13.1 compact specimens; cracks; crack growth; creep; fatigue; metals

ANNEXES

(Mandatory Information)

A1. FUNCTIONAL RELATIONSHIPS

INTRODUCTION

In this Annex, guidance is provided for selecting crack tip parameters for representing creep-fatigue crack growth data from tests conducted using this method. Creep-fatigue crack growth rates are affected by fatigue damage in the form of cyclic plasticity which accumulates with applied cycles and by creep damage in the form grain boundary cavitation or environmental attack, or both, such as oxidation that is time-dependent. Synergistic effects from all three mechanisms can also be a factor in determining the crack growth rates. Under specific circumstances, crack growth rate data may be represented by the linear elastic fracture mechanics parameter, ΔK, or the time-dependent parameter, $(C_t)_{avg}$, as described in section 10.3. The following discussion elaborates these circumstances.

A1.1 *Linear Elastic Fracture Mechanics (LEFM) Approach*:

A1.1.1 The linear elastic fracture mechanics approach for creep-fatigue crack growth relies on ΔK for characterizing the crack growth rate per cycle, da/dN, while keeping the loading frequency and waveform constant. Examples of this relationship are shown in Fig. A1.1 for a creep-ductile material, 304 stainless-steel (**11**) and in Fig. A1.2 for a creep-brittle material, Inconel 718 (**12**). Inconel 718 is susceptible to oxidation enhanced crack growth at elevated temperatures. The waveform employed in both these studies was triangular in which the loading and unloading times are the same. The crack growth rates are clearly dependent on the loading frequency and are quite adequately represented by ΔK. This approach may also be applied to creep-brittle materials when the loading waveform includes a hold-time. An example of such data is shown in Fig. A1.3 for Astroloy (**13**). For creep-ductile materials and loading wave-forms that include hold-times, the crack growth rate per cycle may be represented by ΔK if the conditions of Eq A1.1 and Eq A1.2 are met. In such instances, the data from different hold-times must be identified separately.

A1.1.1.1 *Limitations of LEFM Approach*—When time-dependent strains due to creep in the crack tip region become significant, ΔK loses its uniqueness as the crack tip parameter. To ensure validity of LEFM, the cycle time must be an order of magnitude less than the transition time, t_T, calculated from Eq 15. This condition is expressed as:

$$\frac{1}{F} \le \frac{t_T}{10} \tag{A1.1}$$

where:

F = the loading frequency (the inverse of cycle time).

A1.1.1.2 Only data that meets the above requirement and also satisfies the condition for linear elastic behavior given as follows will be valid by this method:

$$W - a \ge \frac{4}{\pi}\left(\frac{K_{max}}{\sigma_{ys}}\right)^2 \tag{A1.2}$$

A1.2 *Time-dependent Fracture Mechanics Approach*:

A1.2.1 For creep-ductile materials that include a hold-time that accounts for more than 90 % of the cycle time, time-dependent fracture mechanics parameters have been shown to

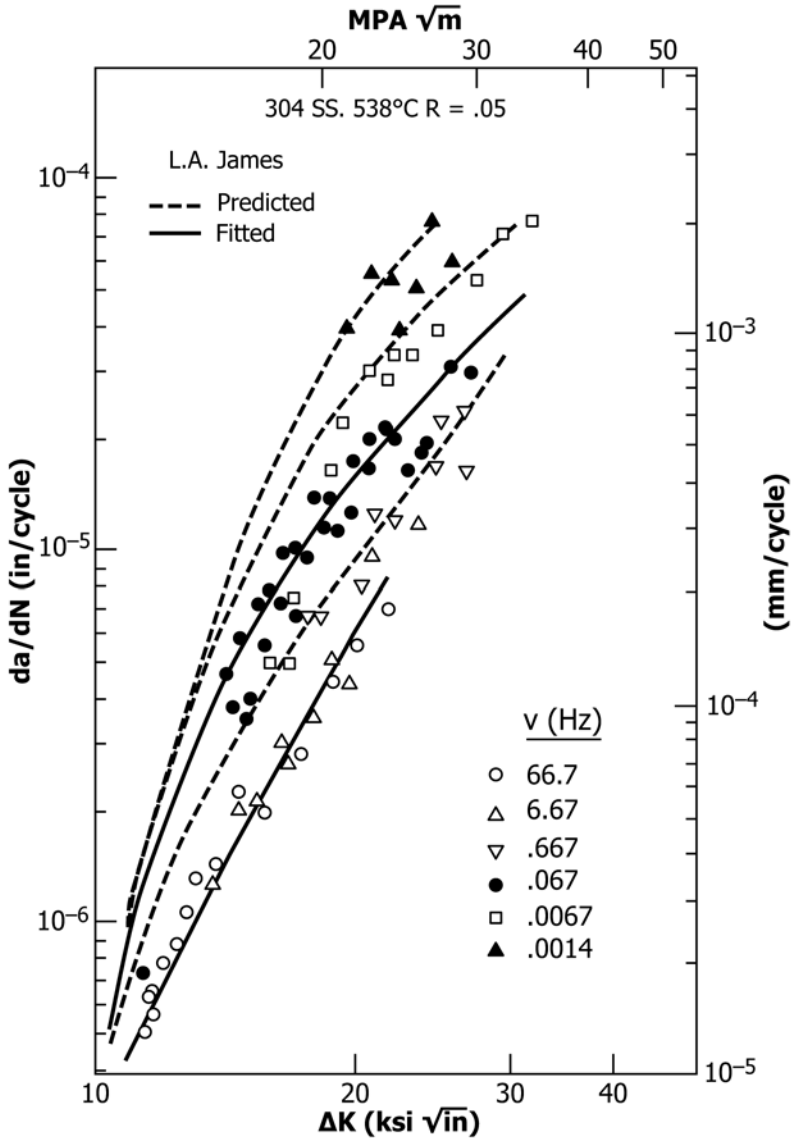

FIG. A1.1 Effect of Loading Frequency *(F)* on the Elevated Temperature Creep-Fatigue Crack Growth Behavior of Creep-Ductile 304 Stainless Steel (11)

be successful in normalizing the hold-time effects. In this approach the average time-rate of crack growth during the cycle is correlated with the average value of the $(C_t)_{avg}$ parameter as shown in Fig. A1.4 (**3**). These tests are usually performed at different hold-times including the condition of zero hold-time. The validity requirements for conducting tests yielding valid data by this method must satisfy the conditions laid out in Eq A1.1 and Eq A1.2.

A1.3 *Creep-Fatigue Crack Growth Models*:

A1.3.1 Models for creep-fatigue interaction can be separated by ones that account for hold-time effects and those that only apply to continuous cycling situations. The objective of these models is to provide the ability to interpolate/extrapolate time-dependent crack growth effects. Linear superposition models have shown to work well for continuous cycling when the *da/dN* for the whole cycle can be characterized by ΔK for a wide range of frequencies. The governing equation for such a model is as follows:

$$\frac{da}{dN} = \left(\frac{da}{dN}\right)_o + \int_{\frac{1}{F_0}}^{\frac{1}{F}} \left(\frac{da}{dt}\right) dt \qquad \text{(A1.3)}$$

where, the first term on the right hand side of Eq A1.3 is the cycle dependent crack growth rate corresponding to a reference frequency, F_0, and F is the frequency of continuous cycles.

A1.3.2 For frequencies greater than F_0, the time-dependent effects are considered negligible in the linear damage summation model. The second term is the time-rate of crack growth integrated over the time-dependent portion of the cycle and is also uniquely related to ΔK. Fig. A1.4a shows data for API Astroloy at 700°C at various loading frequencies (**14**). The

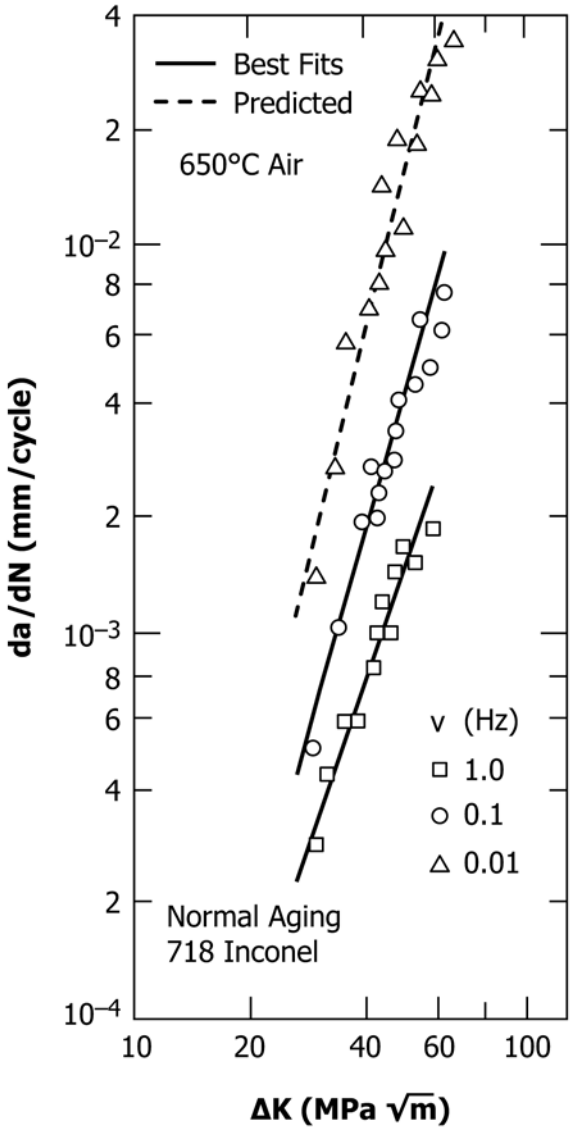

FIG. A1.2 Effect of Frequency *(F)* on the Elevated Temperature Behavior Creep-Fatigue Crack Growth Behavior of Creep-Brittle Inconel 718 (13)

same data for a constant Δ K are plotted as a function of loading frequency in Fig. A1.4b clearly delineating the cycle-dependent and the time-dependent regions and the interaction region (**15**). The plot demonstrates the validity of the linear damage summation approach in accounting for creep-fatigue-environment effects in Ni base alloys (**14, 15**). Similarly, the dotted lines in Fig. A1.1 are predicted trends from the linear damage summation model for 304 stainless-steel (**16**).

A1.3.3 For creep-ductile materials subjected to loads with hold-time, the following equation has been shown in several studies (**2, 3**) to represent creep-fatigue crack growth behavior at a wide range of hold-times as shown in Fig. A1.5 taken from (**3**):

$$\frac{da}{dN} = C_0(\Delta K)^{n_0} + \int_0^{t_h} C_1((C_t)_{avg})^q \, dt \qquad \text{(A1.4)}$$

where, the first term on the right hand side of Eq A1.3 and the constants associated with that term correspond to crack growth rates for pure fatigue cycles (the same as $(da/dN)_0$ in Eq A1.3) and is purely cycle dependent; in other words, continuous cycle conditions with cyclic frequencies of F_0 or greater. The second term is the time-dependent term where the crack growth rate is characterized by the $(C_t)_{avg}$ parameter. The advantage of such an approach is that it seamlessly estimates the creep-fatigue crack growth behavior for short to long hold-times. However, it has only been demonstrated to apply to situations in which hold-time is dominant in the cycle time.

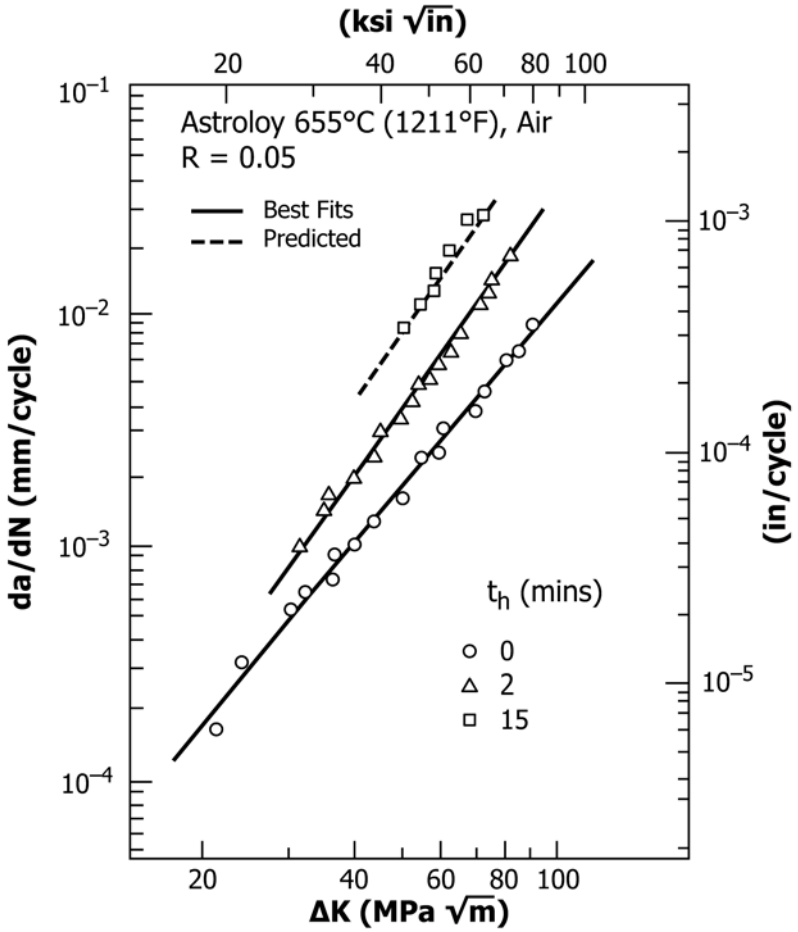

FIG. A1.3 Fatigue Crack Growth Rate Behavior for Astroloy for Waveforms Including Hold-Time (13)

A1.3.4 For creep-brittle materials, in which the time-dependent contributions are also characterized by K, the following equation has been shown to represent the data at various hold-times (**17**). The predicted line in Fig. A1.3 is from this model.

$$\frac{da}{dN} = C_0(\Delta K)^{n_0} + C_2(\Delta K)^{n_2}\sqrt{t_h} \qquad \text{(A1.5)}$$

where, the first term on the right hand side is the time-independent term, the same as in Eq A1.3 and Eq A1.4. The second term includes two constants obtained from regression analysis of the data at one hold-time such as the 2 minute hold-time data in Fig. A1.3. Subsequently, the equation is used to predict the data at other hold-times as shown by the dotted line in Fig. A1.3 for a hold-time of 15 minutes (**17**). The square-root dependency on hold-time in Eq A1.5 is a direct consequence of the assumption that the degradation is controlled by diffusion kinetics of oxygen along the grain boundaries in the crack tip region and the diffusion kinetics follow the parabolic law.

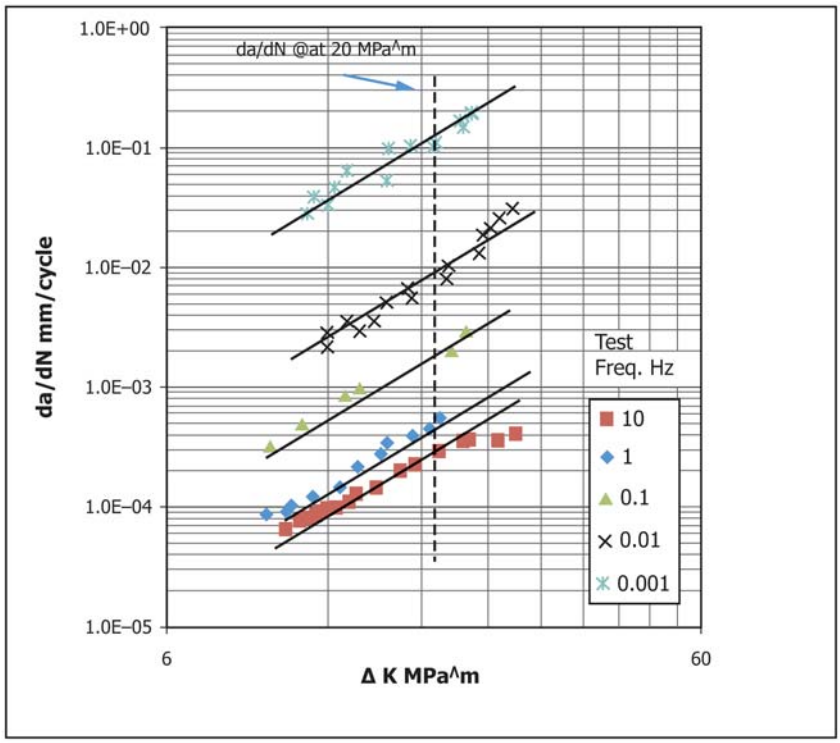

a

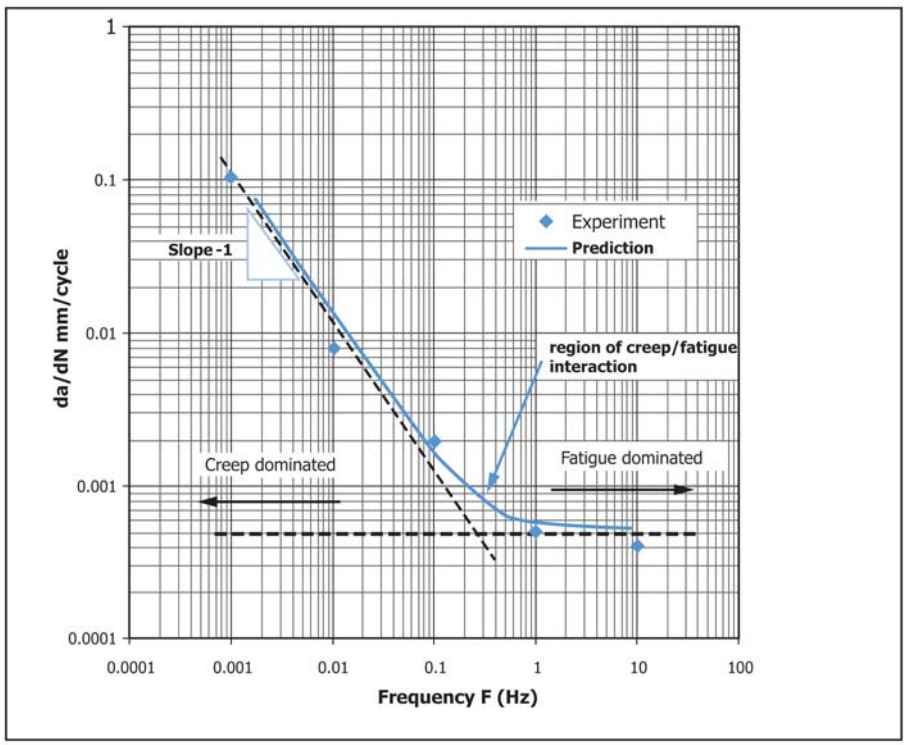

b

FIG. A1.4 Elevated Temperature Fatigue Crack Growth Rate for API Astroloy, a Ni Base Superalloy, at 700 °C (a) as a Function of ΔK for a Wide Range of Loading Frequencies and (b) Crack Growth Rate per Cycle at a Constant Value of ΔK for the Same Lading Frequencies as in (a), Delineating the Fatigue, Creep and Creep-Fatigue Interaction Regimes (14), (15)

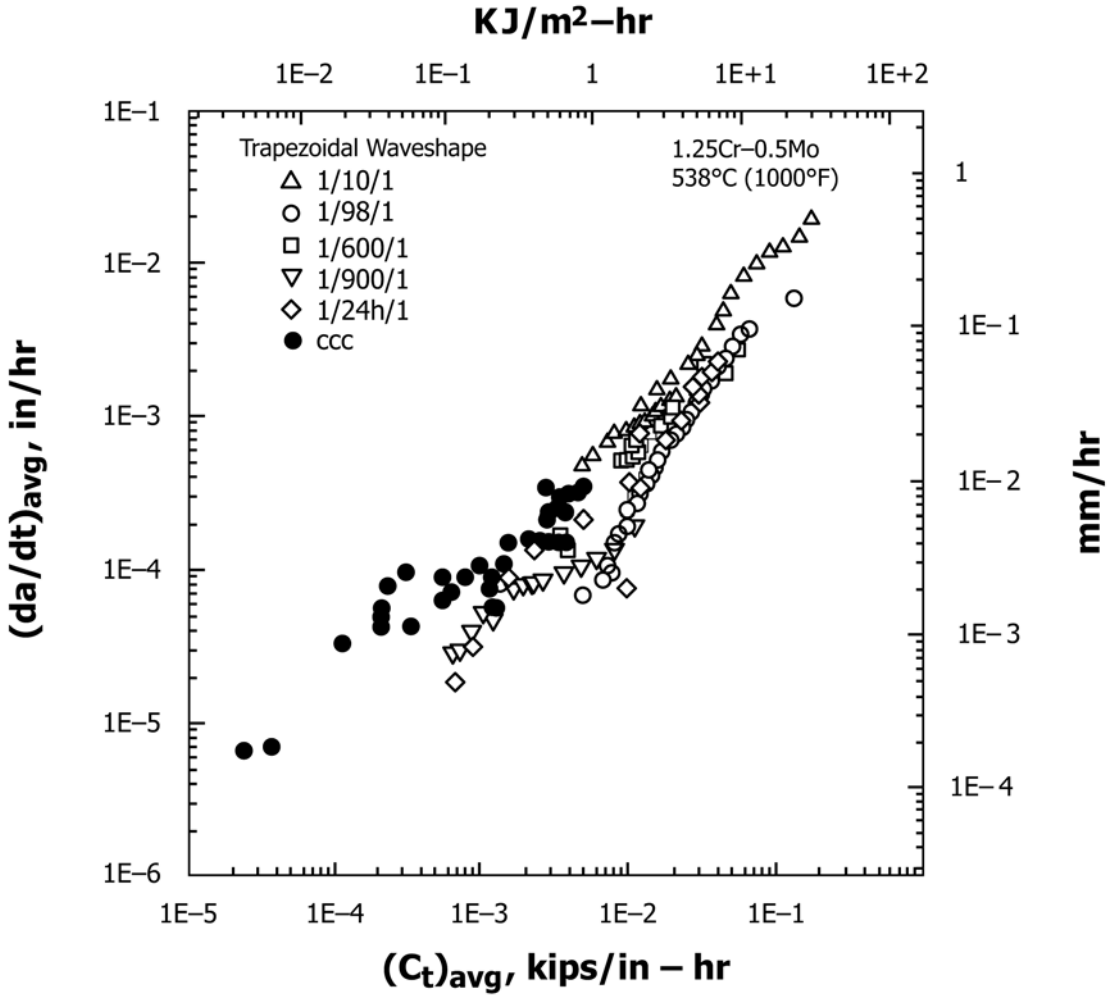

FIG. A1.5 Average Time Rate of Crack Growth During Hold-Time as a Function the Average Value of $(C_t)_{avg}$ for Several Hold-Times Ranging 10 Seconds to 24 Hours and Including Creep Crack Growth Rates for 1.25 Cr -0.5Mo Steel at 538°C (3)

A2. GUIDELINES FOR USE OF ELECTRIC POTENTIAL DIFFERENCE (PD) FOR CRACK SIZE DETERMINATION

A2.1 *Voltage versus Crack Size Relationships for All the Specimens*—The initial and final potential difference (PD) readings correspond to the initial and final crack sizes, respectively, during the test. For the intermediate points, crack size at any instant may be determined by a direct linear interpolation of the PD data corresponding to the measured initial crack size, a_o and final measured crack size, a_f, provided both a_o and a_f can be precisely measured on the fracture surface of the specimen at the end of the test. Thus, the crack size at any instant, a is given by:

$$a = \left[(a_f - a_0) \frac{(U - U_0)}{(U_f - U_0)} \right] + a_0 \qquad \text{(A2.1)}$$

where:

U_0 and U_f = the initial and final potential difference readings, respectively, and

U = the instantaneous potential difference corresponding to the crack size, a.

A2.2 If a_f is unavailable, a predetermined relationship between measured voltage and crack size may be used to determine crack size as a function of time. It is expected that test laboratories will have available to them experimental, numerical or analytical expressions relating crack sizes to the changes in output voltages that apply to their specific specimen

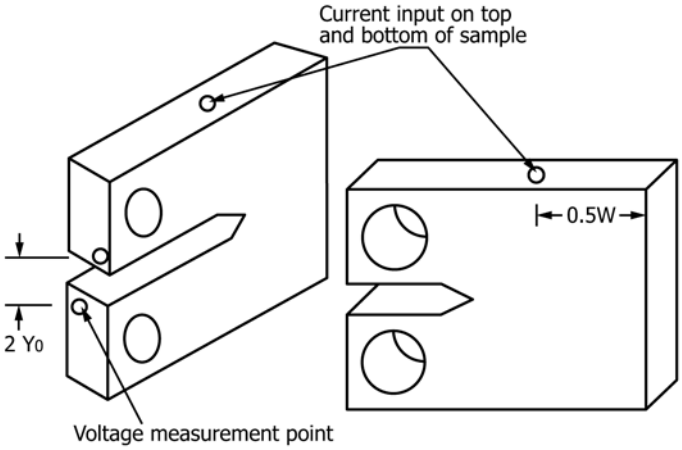

FIG. A2.1 Locations of the Input Current and Output Voltage Leas for C(T) Specimens

geometry and size/input current and output voltage configurations. These relationships will have been verified experimentally to assure their accuracy. For the C(T) specimen, for an input current and voltage lead locations shown in Fig. A2.1, the following closed form equation can be used to compute crack size from measured U/U_0 values:

$$a/W = \frac{2}{\pi}\cos^{-1}\left[\frac{\cosh(\pi Y_0/2W)}{\cosh\left[\frac{U}{U_0}\right]\cosh^{-1}\left\{\frac{\cosh\pi Y_0/2W}{\cos\pi a_0/2W}\right\}}\right] \quad \text{(A2.2)}$$

where:

a_0 = reference crack size with respect to the reference voltage, V_0. Usually, a_0 will be initial crack size, a_0 and V_0 is the initial voltage,
Y_0 = half distance between the output voltage leads, and
U = output voltage.

A2.3 *Measurement of Thermal Voltage for Direct Current Technique*—The voltages U and U_0 used for determining crack size in the equation in A2.1 and A2.2 may be different from their respective indicated readings when using a direct current technique. This difference is due to the thermal voltage, U_{th}, caused by the minor differences in the junction properties or the resistances of the two output leads. An initial measurement of U_{th} is necessary. This can be accomplished by shutting off the current and recording the output voltage. In addition to the initial measurement, a periodic measurement of U_{th} also should be made by shutting off the current for short periods of time during testing. The values of U_{th} must be subtracted from the indicated values of U and U_0 before substituting them in the equation given in A2.1 and A2.2.

NOTE A2.1—The guidelines for use of electric potential difference for crack size determination outlined in the Annex of Test Method E647 are applicable in their entirety for creep-fatigue measurements also. The readers should consult this test method for recommendations on how to use this technique.

A2.3.1 *Discussion*—It should be noted that in some cases the initial PD readings at the beginning of the tests could drop before stabilization and eventually increase with crack extension. Conditions of initial loading, plasticity, excessive creep and damage and crack tip oxidation could affect the extent of this drop in the PD. In such cases, it is recommended that the minimum value of PD attained should be extrapolated back to zero time before crack size determinations are made.

A3. DATA REDUCTION TECHNIQUES

A3.1 The secant or point-to-point technique for computing crack growth rate and deflection rate involves calculating the slope of a straight line connecting two adjacent data points on the a versus N and the V versus t curve during the hold period. It is formally expressed as follows:

$$\left(\frac{da}{dN}\right)_{\bar{a}} = (a_{i+1} - a_i)/(N_{i+1} - N_i) \quad \text{(A3.1)}$$

$$\left(\left(\frac{da}{dt}\right)_{avg}\right)_{\hat{a}} = \frac{1}{t_h}\left(\left(\frac{da}{dN}\right)_{\hat{a}}\right) \quad \text{(A3.2)}$$

$$\left(\left(\frac{dV}{dt}\right)_{avg}\right)_{\bar{N}} = (\Delta V_c/t_h)_{\bar{N}} \quad \text{(A3.3)}$$

where:

$\bar{N}$ = $1/2(N_{i+1} + N_i)$

A3.1.1 The average crack size, $\bar{a} = ½ (a_{i+1} + a_i)$, is used to calculate ΔK and $(C_t)_{avg}$ using Eq 4 and Eq 14, respectively. The term f'/f in Eq 14 is given by (**5**):

$$\frac{f'}{f} = \left[\frac{1}{2+a/W} + \frac{3}{2(1-a/W)}\right] + \left[\frac{\{4.64 - 26.64(a/W) + 44.16(a/W)^2 - 22.4(a/W)^3\}}{\{0.866 + 4.64(a/W) - 13.32(a/W)^2 + 14.72(a/W)^3 - 5.6(a/W)^4\}}\right] \quad \text{(A3.4)}$$

A3.2 When hold-times are too small for reliable changes in force-line-deflection to be measured by the extensometer, the following expression has been to estimate $(C_t)_{avg}$. This expression has been derived for materials that creep in accordance with the power-law, Eq 9 (**3, 8**):

$$(C_t)_{avg} = \frac{2\alpha\beta(1-\nu^2)}{E} F_{cr}(\theta,n) \frac{K_h^4}{W} (f'/f) (EA)^{\frac{2}{n-1}} t_h^{-\frac{n-3}{n-1}} + C^*(t) \quad \text{(A3.5)}$$

$$\text{where, } \alpha = \frac{1}{2\pi}\left(\frac{(n+1)^2}{1.38n}\right)^{\frac{2}{n-1}} \quad \text{(A3.6)}$$

and K_h is the stress intensity parameter during the hold time.

NOTE A3.1—The hold time, t_h, is considered too small for reliable measurement of changes in force-line displacement ΔV when the measured value of ΔV during the hold time is less than five times of the resolution of the force-line-displacement gage as defined in Practice E83. For a Class B2 extensometer, this resolution is less than 0.0001 m/m (in/in). As an example, a class B2 extensometer with a gage length of 12.5 mm will have a resolution of 0.00125 mm or less. Only displacement changes exceeding 0.00625 mm are then considered reliable by this criterion. Clip-on gages that are attached directly to the specimen generally provide more reliable data in comparison to assemblies in which the displacement gage is placed outside the furnace and the force-line displacement is transferred to the gage by rigid rods

A3.2.1 For $\theta = 90°$, the value of $\beta \approx 0.33$ and $F_{cr}(\theta)$ is given in Table A3.1 (**9**). For values of n that are in-between those for which $F_{cr}(\theta)$ is provided in Table A3.1, a linear interpolation can be used.

$$C^*(t) = A(W-a)h_1\left(\frac{a}{W}, n\right)\left(\frac{P}{1.455\eta_1 B(W-a)}\right)^{n+1} \quad \text{(A3.7)}$$

where:

A = pre-exponent constant in power-law creep.

$$\eta_1 = \left[\left(\frac{2a}{W-a}\right)^2 + 2\left(\frac{2a}{W-a}\right) + 2\right]^{\frac{1}{2}} - \left[\left(\frac{2a}{W-a}\right) + 1\right] \quad \text{(A3.8)}$$

A3.2.2 $h_1(a/W, n)$ for various values of a/W and n are listed in Table A3.2 for C(T) specimens.

TABLE A3.1 The Values of F_{cr} as a Function of the Creep Exponent, n (9)

n	3	5	10	13
$F_{cr}(90°,n)$	0.276	0.362	0.4	0.425

TABLE A3.2 The Values of h_1 for C(T) Specimens (18)

	n								
a/W ↓	1	2	3	5	7	10	13	16	20
0.25	2.23	2.05	1.78	1.48	1.33	1.26	1.25	1.32	1.57
0.375	2.15	1.72	1.39	0.970	0.693	0.443	0.276	0.176	0.098
0.5	1.94	1.51	1.24	0.919	0.685	0.461	0.314	0.216	0.132
0.625	1.76	1.45	1.24	0.974	0.752	0.602	0.459	0.347	0.248
0.75	1.71	1.42	1.26	1.033	0.864	0.717	0.575	0.448	0.345
≈ 1	1.57	1.45	1.35	1.18	1.08	0.95	0.85	0.73	0.630

REFERENCES

(1) Saxena, A., *Nonlinear Fracture Mechanics for Engineers*, Boca Raton, FL, CRC Press, 1998.

(2) Saxena, A. and Gieseke, B., Transients in Elevated Temperature Crack Growth, International Seminar on High Temperature Fracture Mechanisms and Mechanics III, EGF-6, Dourdon : s.n., 1987 , pp. 19-36.

(3) Yoon, K. B., Saxena, A., and Liaw, P. K., *Characterization of Creep-Fatigue Crack Growth Behavior Under Trapezoidal Loading*, Vol. 59, 1993, pp. 95-114.

(4) Landes, J. D. and Begley, J. A., A Fracture Mechanics Approach to Creep Crack Growth. Mechanics of Crack Growth, Philadelphia: American Society for Testing and Materials, 1976, pp. 128-148.

(5) Saxena, A., *Creep Crack Growth Under Non Steady-State Conditions. Fracture Mechanics*: Seventeenth Volume, ASTMSTP 905, Philadelphia: ASTM, 1986 , pp. 185-201.

(6) Saxena, A., Ernst, H. A., and Landes, J. D., Creep Crack Growth Behavior in 316 Stainless Steel at 594 °C, *International Journal of Fracture*, 1983, Vol. 23, pp. 245-257.

(7) Bassani, J. L., Hawk, D. E., and Saxena, A., Evaluation of the Ct Parameter for Characterizing Creep Crack Growth in the Transient Regime, *Nonlinear Fracture Mechanics: Time-Dependent Fracture Mechanics*, Vol. 1, ASTM STP 995, Philadelphia: American Society for Testing and Materials, 1989, pp. 141-158.

(8) Adefris, N., Saxena, A., and McDowell, D. L., An Alternative Analytical Approximation of the C_t Parameter, *Fatigue and Fracture of Engineering Materials and Structures*, Vol. 21, 1998, pp. 375-386.

(9) Riedel, H. and Rice, J. R., Tensile Cracks in Creeping Solids, Fracture Mechanics, Twelfth Conference, ASTM STP 700, Philadelphia: American Society for Testing and Materials, 1980, pp. 112-130.

(10) Saxena, A. and Hudak, S. J. Jr., Review and Extension of Compliance Information for Common Crack Growth Specimens, *Int. Journal of Fracture*, 1978, pp. 453-468.

(11) James, L. A., The Effect of Frequency Upon the Fatigue Crack Growth of Type 304 Stainless Steel at 1000F, Stress Analysis of Growth of Cracks, ASTM STP 513, Philadelphia: American Society for Testing and Materials, 1972, pp. 218-229.

(12) Floreen, S. and Kane, R. H., An Investigation of Creep-Fatigue-Environment Interactions in Ni Base Super-Alloy, Fatigue of Engineering Materials and Structures, 1980, Vol. 2, pp. 401-412.

(13) Pelloux, R. M. and Huang, J. S., Creep-Fatigue-Environment Interactions in Astrolloy, R. M. Pelloux and Stoloff, Editors, *Creep-Fatigue-Environment Interactions*, Warrandale, PA, TMS-AIME, 1980, pp. 151-164.

(14) Winstone, M. R., Nikbin, K. M., and Webster, G. A., Modes of Failures Under Creep/Fatigue Loading of Ni-Based Superalloy, *Journal of Materials Science*, 1985, Vol. 20, pp. 2471-2476.

(15) Nikbin, K. M., Webster, G. A., Prediction of Crack Growth under Creep-Fatigue Loading Condition, in Low-Cycle Fatigue, Eds., H. D. Solomon, G. R. Halford, L. R. Kaisand and, B. N. Leis, ASTM STP 942, 1987, pp. 281-292.

(16) Saxena, A., A Model for Predicting the Effect of Frequency on Fatigue Crack Growth Behavior at Elevated Temperature, pp. 247-255, Fatigue of Engineering Materials and Structures, 1981, Vol. 3, pp. 2471-2476.

(17) Saxena, A., A Model for Predicting the Environment Enhanced Fatigue Crack Growth Behavior at High Temperature, Thermal and Environmental Effects in Fatigue: Research–Design Interface–PVP , Vol. 71, Editors: C. E. Jaske, S. J. Hudak, and M. E. Mayfield, ASME, 1984 , pp. 171-184.

(18) Kumar, V., German, M. D., and Shih, C. F., An Engineering Approach for Elastic-Plastic Fracture Analysis, EPRI Report NP-1931, Palo Alto: Electric Power Research Institute, 1981.